INT. J. REMOTE SENSING, 2003, VOL. 24, NO. 5, 1009–1027

An integrative classification of vegetation in China based on NOAA AVHRR and vegetation–climate indices of the Holdridge life zone

Y. PAN†, X. LI†, P. GONG‡, C. HE†, P. SHI† and R. PU‡

†Institute of Resource Science, Beijing Normal University, Key Laboratory of Environmental Change and Natural Disaster of Beijing Normal University, Beijing, 100875, China
‡Center for Assessment and Monitoring of Forest and Environmental Resources, University of California at Berkeley, CA 74720, USA

(*Received 27 September 2000; in final form 9 October 2001*)

Abstract. We developed a method for integrated analysis of multi-source data for vegetation classification at the continental scale, and applied it to China. Multi-temporal 1 km NOAA Advanced Very High Resolution Radiometer (AVHRR) Holdridge's life zone system and its vegetation–climate classification indices such as bio-temperature (BT), potential evapotranspiration rate (PER) and precipitation (*P*) correspond better with undisturbed vegetation types all over the world. We generated 1 km images of BT, PER and *P* using the quantitative model of Holdridge's life zone system with climate data of China. They were processed with principal component analysis (PCA) to produce an ancillary image. This image and 12 monthly images of maximum Normalized Difference Vegetation Index (NDVI) values at 1 km resolution were input into an ISODATA clustering algorithm to carry out a vegetation classification. As a result, 47 information classes were obtained. Seasonal NDVI parameters derived through time series analysis (TSA) of the NDVI temporal profile and a set of quantitative vegetation–climate parameters of Holdrige's life zone model were synthetically utilized to label information classes. In this method, climate, terrain and spectral data were integrated; separability between vegetation types and classification accuracy were improved. A total of 47 land cover classes were obtained. Validation data collected in the field using GPS indicated that an overall classification accuracy of 71.4% was reached, an 8.1% improvement to the map derived only from multi-temporal NDVI images. To compare our results with the International Geosphere–Biosphere Programme (IGBP) DISCover land cover dataset, we aggregated our land cover classes according to the IGBP classification system. The overall classification accuracy for the aggregated vegetation map from our classification results improved IGBP land cover map from 75.5% to 86.3%.

1. Introduction

Global, continental and regional land cover data are essential to global change research (Loveland *et al.* 2000). There is considerable ignorance concerning the global distribution of vegetation types. This is an issue of increasing concern (IGBP 1990, Townshend 1991). Reliable, georeferenced data on global vegetation cover is a basic requirement to the modelling of the earth system (IGBP 1992). Only satellite sensor data can provide us with a truly synoptic view of the earth that may potentially

International Journal of Remote Sensing
ISSN 0143-1161 print/ISSN 1366-5901 online © 2003 Taylor & Francis Ltd
http://www.tandf.co.uk/journals
DOI: 10.1080/01431160110115816

increase the quality, internal consistency, and reproducibility of global land cover information (Townshend *et al.* 1991) and allow us to study the earth as a whole system (Asrar and Dozier 1994, Kramer 1994).

National Oceanic and Atmospheric Administration (NOAA) Advanced Very High Resolution Radiometer (AVHRR) data have proven to be a valuable data source for study of global, continental and regional land cover and long-term terrestrial monitoring (IGBP 1992, Townshend 1994). One kilometre AVHRR data have been suggested by the International Geosphere–Biosphere Programme (IGBP) to be the most appropriate for the generation of a science-quality global land cover database (Loveland *et al.* 2000). Normalized Difference Vegetation Index (NDVI), calculated as $NDVI=(CH2-CH1)/(CH2+CH1)$, where CH1 and CH2 represent radiances from channels 1 (0.58–0.68 μm) and 2 (0.725–1.10 μm) of the AVHRR, respectively, is correlated with photosynthetic activities of vegetation and provides an indication of the 'greenness' of vegetation (Sellers 1985). In addition, NDVI is also the most widely employed vegetation index and has proven to be useful in large scale vegetation monitoring. NDVI is broadly correlated in turn with several biophysical parameters such as the level of photosynthetic activity, transpiration rates (Sellers 1985), the fraction of absorbed photosynthetically active radiation (FPAR), evapotranspiration (Running and Nemani 1988, Goward and Hope 1989), biomass of green leaf (Box *et al.* 1989), leaf area index (LAI), net primary production (NPP) (Tucker and Sellers 1987, Prince 1991, Potter *et al.* 1993, Ruimy *et al.* 1994) and CO_2 flux (Box *et al.* 1989).

During the past 10–15 years, substantial progress has been made in using NOAA AVHRR data for land cover characterization. For example, supervised classification (e.g. Tucker *et al.* 1985, Townshend *et al.* 1987, DeFries and Townshend 1994, DeFries *et al.* 1998a) or logical classification systems (e.g. Running *et al.* 1995), unsupervised classification (e.g. Achard and Estreguil 1995, Driese *et al.* 1997), and a mixed approach (i.e. Loveland *et al.* 1991, 1995, Loveland and Belward 1997), in which an initial non-hierarchical and unsupervised classification was subsequently refined by a supervised reassignment according to mapped non-satellite environmental information, were utilized in land cover classification. In recent years, numerous variations have been developed (Cihlar 2000). For example, decision trees, neural networks, fuzzy classification and mixture modelling for supervised classification; and classification by progressive generalization, classification through enhancement, hierarchical approach and post-processing adjustments for unsupervised techniques have been proposed. Some of them were applied in global, continental or regional land cover classifications (Hansen *et al.* 1996, 2000, DeFries *et al.* 1998b, Cihlar *et al.* 1998). Many of them have not yet been used at large scale. Independent ground information is required by both the supervised and unsupervised methods (Cihlar 2000) for accuracy assessment of classification results.

It is difficult to only use remotely sensed data to classify land cover types. Metrics such as maximum NDVI, length of growing season derived from a temporal profile of 10 day or monthly NDVI valves, rather than directly from the images themselves were used by DeFries *et al.* (1995b), while, in some cases, additional AVHRR data, multi-resolution imagery and integrated analysis method were included along with NDVI for land classification (Lambin and Ehrlich 1995, Cihlar *et al.* 1996, Laporte *et al.* 1998, Moody 1998). Multi-source data such as elevation, eco-regions, climate and soil, etc. were considered as important ancillary information for land cover classification (Loveland *et al.* 1991, Brown *et al.* 1993). In general, these ancillary

data were employed in post-classification in order to split the heterogeneous preliminary greenness classes into relatively homogeneous land cover regions (Eidenshink 1992, Loveland *et al.* 1997, 2000). Although global land cover datasets derived from AVHRR data are currently available (IGBP Data and Information System (IGBP-DIS) DISCover and University of Maryland (UMd) 1 km land cover maps) (Hansen and Reed 2000), methods for deriving land cover from the satellite sensor data are still being developed (Loveland *et al.* 2000).

Vegetation types and their patterns are mainly controlled by climate and topography. Every climate type or region has a set of corresponding vegetation types. Coupling relationship and bio-climate diagram between climate and vegetation was developed in the past century by many researchers, in order to predict vegetation patterns by using climate indices and inversely to deduce future and past climates according to vegetation distributions. There are many kinds of climate–vegetation classification methods. For example, Penman (1956), Thornthwaite (1948), Holdridge (1947) and Kira (Xu 1985) developed quantitative relationships residing in climate and vegetation. These methods defined a potential vegetation type according to either some climate indices (e.g. temperature and precipitation, etc.) or an integrated climate index: Potential Evapo-transpiration (PE), which is used widely in analysis of vegetation–climate relationships and classification. PE is also an important parameter in regionalization of vegetation and quantitative interpretation of environment. According to Penman's definition, PE includes evaporation from all kinds of surfaces and transpiration of plant. Different PE calculations were developed in different regions in the world, and they must be adjusted when utilized in other regions. Among them, Holdridge's life zone classification system was used widely because it has a close relationship between its compendious, reasonable indices and distribution of vegetation types, i.e. vegetation types can be estimated and patterns of biome can be denoted according to climate indices in a certain region using this method (Holdridge 1947).

The objective of this study is to explore a new method of vegetation classification at large spatial scales with a specific application to China (figure 1). We used multi-temporal 1 km NOAA AVHRR NDVI images that reflect conditions and seasonal rhythm of vegetation on land, and integrative climate–vegetation indices derived from Holdridge's life zone system in the classification of vegetation. We assessed the classification results using data collected from field visits (regions enclosed by broken line in figure 1) and various ancillary data sources.

2. Holdridge's life zone and vegetation patterns in China

2.1. *Holdridge's PE indices and their eco-geographical significance*

Holdridge's life zone classification system is widely used in the world due to its simplicity and convenience for calculation of indices and better correspondence with vegetation types. Recently it has been applied to assess environment, engaged in ecological regionalization and predicted the impact of global change on ecosystems (Chang 1993). Combination of plant communities can be confined based on three basic climate variables: temperature, precipitation and humidity. This kind of combination is named 'life zone'. Life zone has two meanings: a definite vegetation type and a range of temperature and precipitation that gives birth to a vegetation type. It is a synthetic exhibition of zones of heat quantity and zones of humidity. In this way, the potential of vegetation types occurring in a particular region can be defined according to climate records. Inversely, regional climate conditions can also be

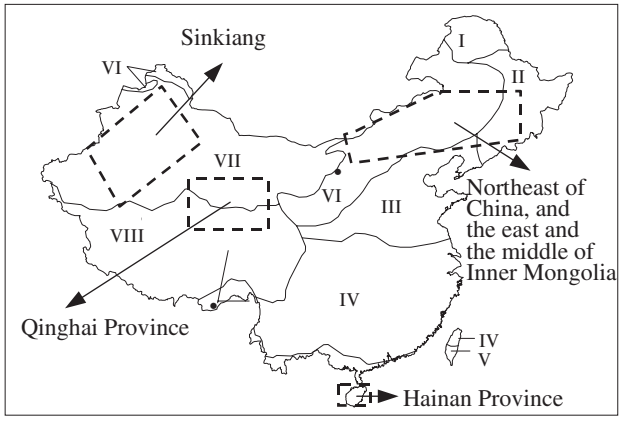

Figure 1. Map of study area. I—cool temperate conifer forest region; II—temperate conifer–broadleaf mixed forest region; III—warm temperate deciduous broadleaf forest region; IV—subtropical evergreen broadleaf forest region; V—tropical monsoon forest and rain forest region; VI—temperate grassland region; VII—temperate desert region; VIII—Qinghai–Tibet Plateau high and cold vegetation region. Dashed boxes are areas where field visits are made.

confirmed by plant communities observed in the field (Holdridge 1947, Chang *et al.* 1993).

Indices of Holdridge's life zone are bio-temperature (BT), precipitation (P) and potential evapotranspiration rate (PER). The mean annual BT is considered as an index of energy. In general, it varies from 0°C to 30°C. Mean daily temperature outside this range (i.e. >30°C and <0°C) is foreclosed. BT can be calculated with:

$$\mathrm{BT} = \Sigma t/365 \tag{1}$$

or

$$\mathrm{BT} = \Sigma T/12 \tag{2}$$

where BT represents the mean annual bio-temperature (°C), t the mean daily temperature ($0^\circ\mathrm{C} < t < 30^\circ\mathrm{C}$), and T the monthly average temperature ($0^\circ\mathrm{C} < T < 30^\circ\mathrm{C}$).

Potential evapotranspiration (PET) and its ratio to precipitation, namely potential evapotranspiration rate (PER), was defined by Holdridge based on experimental data through the following equations:

$$\mathrm{PET} = \mathrm{BT} \times 58.93 \tag{3}$$

$$\mathrm{PER} = \mathrm{PET}/P = \mathrm{BT} \times 58.93/P \tag{4}$$

where P is annual precipitation (mm).

2.2. *Zonal vegetation types and patterns in China*

Vegetation patterns present horizontal zones along latitudes in eastern China, which from north to south are divided into coniferous forest, deciduous broadleaf forest, coniferous–deciduous mixed forest, evergreen broadleaf forest and monsoon rain forest, and rainforest. The general characteristics of climate are humid in south-east China, arid in north-west China, and semi-arid in between. Horizontal zones of vegetation in the latitude direction are also obvious, which are divided into forest,

grassland and desert from the south-east to the north-west. Of the most prominent and the biggest in the world is the Qinghai–Tibet Plateau located on the south-west of China. A series of high and cold vegetation types of subtropical and temperate, including meadow, grassland, shrub and desert, grow there (Wu *et al.* 1980).

2.3. *Holdridge's PE indices and their relation to vegetation in China*

An equilateral triangle constructed by BT, *P* and PER was adopted to define conditions of various vegetation types; quantitative relationships between vegetation types and their climate conditions could be found and the life zone could be compartmentalized based on the diagram (Holdridge 1967). A valuable supplement to Holdridge's life zone classification and a diagram have been done, that is mainly representative of high and cold zones (e.g. in high mountain and high latitude zone) and borders between warm temperate zone and subtropical zone. The result is more suitable to vegetation regionalization in China (figure 2) (Chang *et al.* 1993). It is also obvious that the spatial patterns of zonal vegetation types or biomes are preferably represented by Holdridge's life zone classification in China. Consequently, it is possible for us to define the regional climate–vegetation types using its climate indices: mean monthly temperature and annual precipitation through this system.

3. Data sources

3.1. *NOAA AVHRR NDVI data*

Initial experiments using 1989 biweekly NDVI composites of the western USA suggested that the utilization of monthly composites would both minimize data volume and computational time without unduly affecting results (Loveland *et al.* 1991). Used in this study are 1 km monthly NOAA AVHRR NDVI data spanning a 12-month period (April 1992–March 1993). All NDVI data were scaled to 8 bits,

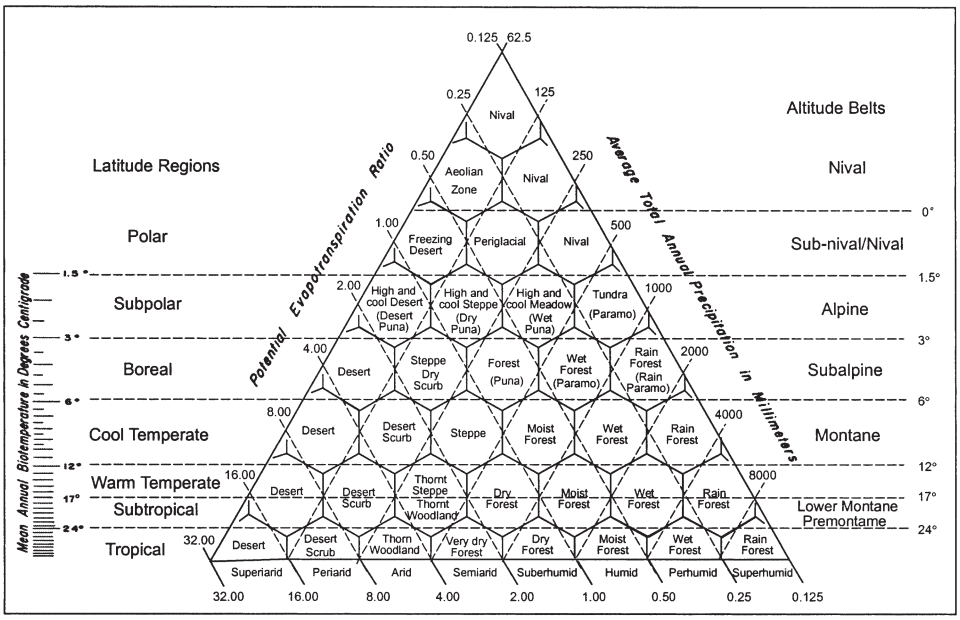

Figure 2. A supplement to Holdridge's life zone classification and diagram (Chang *et al.* 1993).

and geo-registered to Lambert Azimuthal Equal Area map projection whose standard parallel is 45° N and central meridian is 100° E.

3.2. *Climate data*

Monthly climate data derived from 658 climate stations in China in the same period as the NOAA images include total monthly precipitation, mean monthly temperature, wind speed, percentage of day light hours, water vapour pressure. These data were provided by the Climate Center of Weather Bureau of China.

3.3. *Digital Elevation Model (DEM) data*

The DEM data with the same projection and spatial resolution as NDVI images were subset out of the global digital elevation model compiled by the USGS EROS Data Center.

3.4. *Other data*

Other ancillary maps, including published provincial, national vegetation maps at different scales, national land use map at 1:1 000 000 scale (Wu 1990), land cover maps, forest, desert and steppe distribution map, crop calendar map, climate distribution maps, etc., were gathered for use in the interpretation phase of the study and served as reference data to guide us labelling the clustering results.

4. Methods

4.1. *Create digital images of Holdridge's life zone indices*

One kilometre maps of latitude and longitude covering China were produced in the same projection as NDVI images and the DEM. Many previous studies have indicated that BT, as an index of energy, is determinately correlated to latitude, longitude and elevation in China (Chang *et al.* 1989). Therefore, we used a multiple regression method to calculate BT:

$$\mathrm{BT} = 432.06 - 4.90L_{\mathrm{a}} - 0.97L_{\mathrm{o}} - 0.037E \tag{5}$$

(coefficient of correlation $R = 0.98$, Number of samples $n = 658$), where L_{a} stands for latitude, L_{o} for Longitude and E for elevation.

All maps, latitude, longitude and DEM, were integrated to derive the BT map. PER map was created based on equations 3 and 4 using calculated BT map and P map. The P map was derived through interpolation of data at the 658 climate stations using a kriging method. Due to the limited number of climate stations over the entire China, interpolated precipitation can only represent the macro-trend. This is helpful in broad-scale vegetation classification. Because topographic data are helpful in precipitation modelling at local scale and thus may introduce unnecessary details for vegetation classification, we did not use topographic data in the interpolation.

4.2. *Integration of multi-source data and unsupervised classification*

Principal Component Analysis (PCA) has been used successfully in data transformation of remote sensing images, data compression and change detection. This method has proven to be effective in reducing the number of data dimension for classification, especially in change detection (Tucker *et al.* 1985, Fung and LeDrew 1987, Townshend *et al.* 1987, Eastman and Fulk 1993, Gong 1993). The three image layers of PER, BT and P were input to PCA to generate the first component image

(PC1) for classification. PC1 accounts for 93.4% of the total variance. Therefore, including only PC1 in the classification would reduce data dimension while preserving most of the information necessary for classification. The 12-monthly NDVI composites and the PC1 image were clustered using the Iterative Self-Organizing Data Analysis Technique A (ISODATA) algorithm in ERDAS IMAGINE 8.31. With a convergence threshold set to 98%, the algorithm iterated 12 times. Unsupervised classification uses clustering to identify 'natural' groupings of pixels with similar spectral properties of vegetation. Spectral regions defined using an unsupervised strategy can be treated as classic geographic regions and can serve as models of local landscape diversity (Loveland *et al.* 2000).

4.3. *Profile parameter extraction*

Profile algorithm was applied to multi-temporal NDVI images to characterize the temporal change of plant growth. The image of clustering results was used as a mask while the multi-temporal NDVI images were used to construct profiles. A number of characteristic parameters for each vegetation type, such as the mean, maximum, minimum, standard deviation, variance, etc. were calculated from the profiles, and these parameters allowed us to analyse the differences among various vegetation types.

4.4. *Confirmation of vegetation types based on information classes and vegetation characterization*

The Vegetation Map of China at a scale of 1:4 000 000, compiled by the Compilation Committee of 'Vegetation of China', was adopted to act as a base on which the information classes were confirmed and interpreted. Then, an integrative analysis of the profile for each type, the results from TSA, the index parameters from Holdridge's life zone system, and various ancillary data mentioned in §3. Meanwhile, information classes obtained from ISODATA were labelled at the regional scale according to the available ancillary digital and analogue data. Finally, vegetation types were named and characterized.

4.5. *Validation of classification and comparison with other maps*

The result of classification was validated based on field verification located by GPS. Due to the limitation of time and financial resources, field sites were only chosen from the north-east of China, the east and the middle of Inner Mongolia, Qinghai Province, Sinkiang, and Hainan Province (figure 1). According to the vegetation classification result and other ancillary maps, such as vegetation map, topographic map, the routes were preliminarily designed to cover as many distribution regions of zonal vegetation types as we could. Two kinds of sampling methods were adopted with GPS. One was equal distance sampling, in which field sampling plots were assigned every 25 km. The other was intentional sampling, in which the plots were positioned according to distribution area of zonal vegetation types in field. In this way, the smaller the area was (e.g. in ecotone), the denser the plots were set. In every plot, latitude, longitude, elevation, landform, land cover types, dominant species of plant communities, landscape structure and estimated proportions of different elements, land use conditions were recorded.

The result of classification was then compared with the results from two other sources, the result of classification using the 12 monthly NDVI images only and the

IGBP DISCover land cover dataset (Loveland *et al.* 2000). Their accuracies were checked against field visit data.

5. Results and analysis

5.1. *Holdridge's life zone indices and the first component image*

Figure 3(*a*) clearly shows that the regional patterns of BT distribution from the north to the south in China. Where there is a higher BT and a lower *P*, a larger PER will occur. For example, PER in Tulufan Basin in Sinkiang reaches its highest value in China because of its high BT and low *P* (figure 3(*b*)).

5.2. *Integrative analysis based on both seasonal NDVI rhythm and Holdridge's life zone indices*

Time Series Analysis (TSA) based on seasonal rhythm of vegetation growth represented by NDVI (DeFries *et al.* 1994) was carried out by applying the profile algorithm. Monthly NDVI temporal series for various information classes were shown in figure 4. Meanwhile, the means and variances of BT, *P* and PER for each information class were also calculated and used as ancillary data (as an example, the means and variances of BT, *P* and PER of classes 28 and 29 are listed in table 1) to quantitatively distinguish various information classes.

In figure 4, the difference of seasonal characteristics of NDVI among many information classes is not sufficiently clear. Because the indices of Holdridge's life

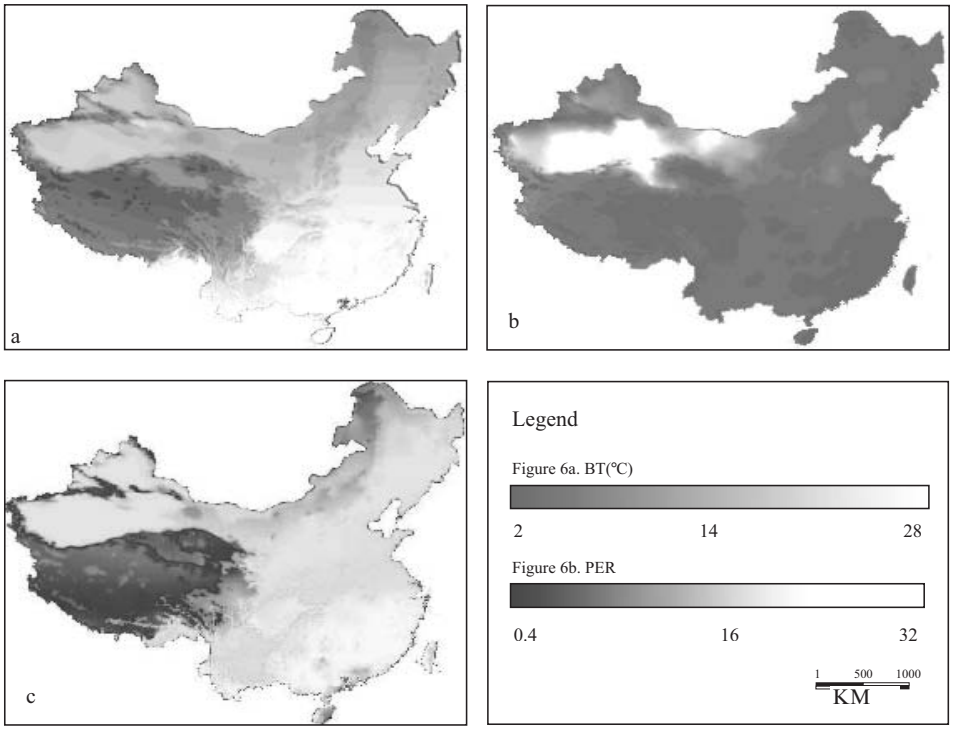

Figure 3. Holdridge's life zone indices and PC1 image. (*a*) BT spatial distribution in China; (*b*) PER spatial distribution in China; (*c*) the PC1 image, which accounted for a 93.4% of the total variance, was chosen to act as an element of the classification vector.

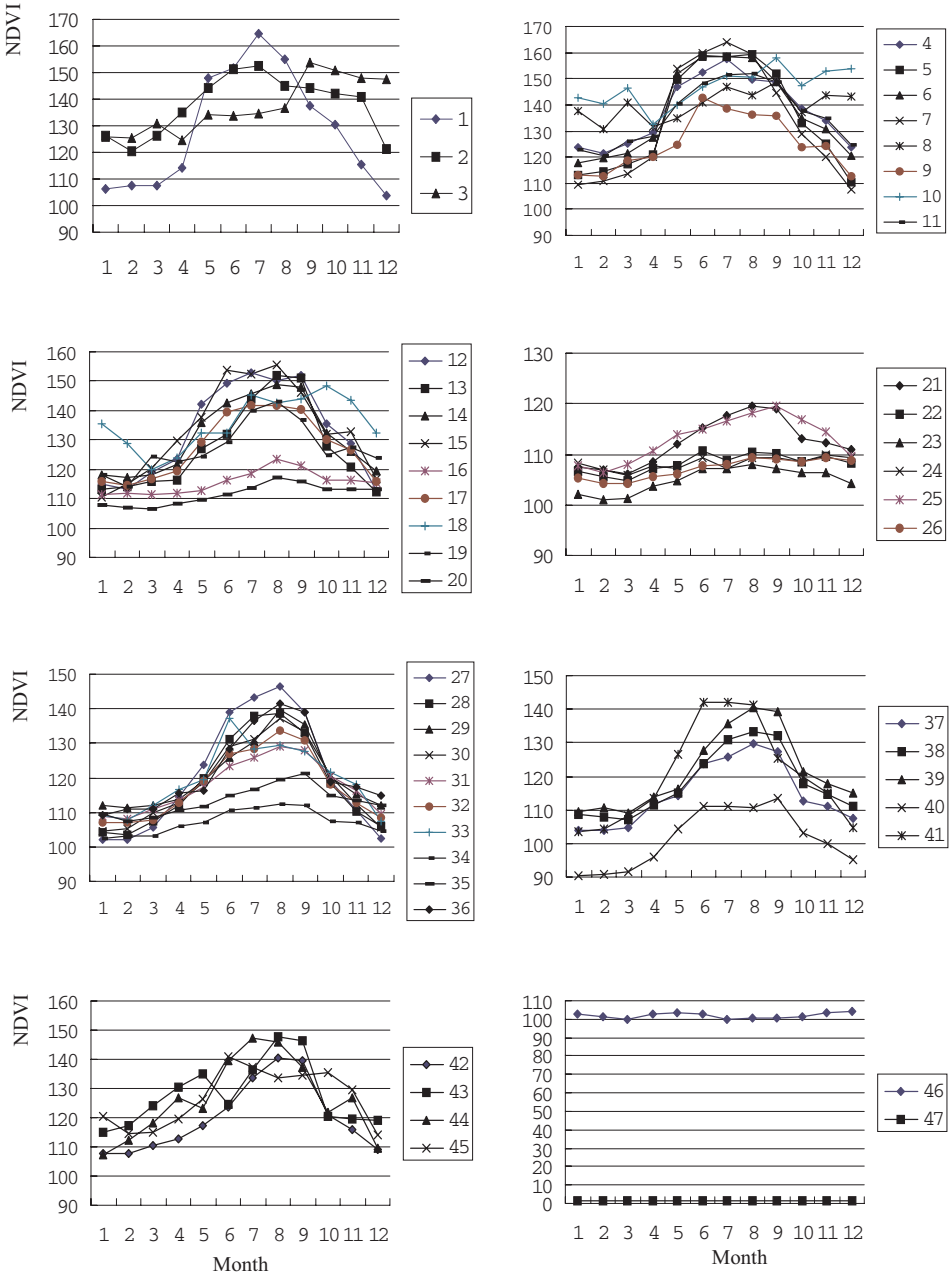

Figure 4. Seasonal NDVI rhythms from the 47 information classes.

zone were markedly different among some similar classes, such data (e.g. in table 1) should be useful in distinguishing information classes. For example, although nos 28 and 29 have similar seasonal NDVI characteristics (figure 5), there are different dominant species of plant community in regions occupied by the two classes. No. 28 is *Filifolium sibiricum* while no. 29 is Single crop + *Stipa baicalensis*/*Bothriochloa ischaemum, Themeda triandra*. From table 1, however, the difference between their

Table 1. Example indices of Holdridge's life zone system for different types.

	BT		*P*		PER	
Code	Mean	Variance	Mean	Variance	Mean	Variance
28	9.797	2.805	357.462	173.089	2.175	6.826
29	11.740	2.943	410.522	192.593	1.676	2.332

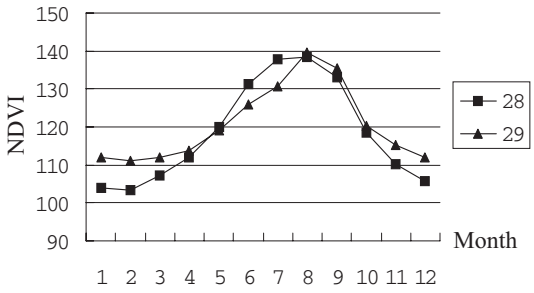

Figure 5. Seasonal rhythm of NDVI from information classes nos 28 and 29.

means and variances of Holdridge's life zone indices can be easily seen. Therefore, the indices of Holdridge's life zone derived from climate parameters were combined with spectral–temporal information of vegetation extracted from remotely sensed data to improve classification accuracy.

5.3. *Final vegetation classification result*

The final vegetation map shows clearly the horizontal zones along the gradient of precipitation from south-east to north-west and the gradient of temperature from north to south in China (figure 6). Under the support of many kinds of ancillary information, such as published vegetation maps, climate region maps, crop calendar and distribution map, land use map, forest, desert and steppe distribution maps (all of them are in digital format), and the digital elevation map, the information classes were named according to the naming rule of 'Vegetation of China' (Wu *et al.* 1980) (table 2). Finally, vegetation types were confirmed and/or modified according to field survey.

5.4. *Assessment of classification accuracy*

Results of field validation (table 3) show that the accuracies in north China (the north-east of China, the east and the middle of Inner Mongolia, Qinghai Province, Sinkiang) were better than that in regions in the south of China (Hainan Province). The average accuracy in the north was 73.3%, in the south was 67.5%, and the average accuracy of all field plots was 71.4%. This seems to be reasonable as the level of vegetation heterogeneity is generally higher in south China than in the north. Errors mainly occurred in regions of various shrub vegetation types. It was difficult to distinguish them from cropland and broadleaf forest, especially in mixed regions of cropland with natural vegetation; or appeared in ecotones of two or more vegetation types recorded as mixed pixels on NOAA AVHRR imagery. Meanwhile, we also produced a vegetation classification map using only 12 monthly NDVI images in order to test whether the PC1 employed can improve classification accuracy. As

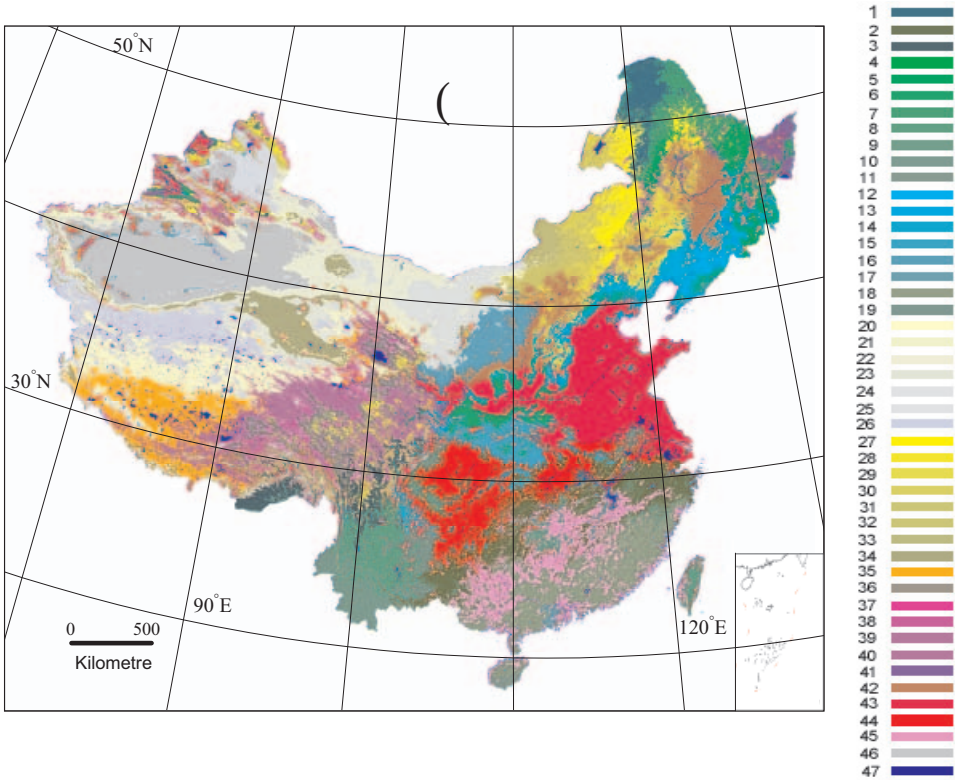

Figure 6. The map of vegetation types in China.

expected, the result showed much more mixed types when compared to the result with the inclusion of PC1. For example, cropland, shrub and grassland, and shrub, short forest, broadleaf forest and mixed forest cannot be separated easily in many regions. The average accuracy is only 63.3%. To our knowledge, this study is for the first time reporting partially validated results of vegetation classification for China.

5.5. *Cross-walk to IGBP DISCover global land cover system*

In order to compare our classification results with those of the IGBP DISCover land cover classification system (Hansen *et al.* 2000), the categories in this study listed in table 2 were aggregated with reference to the definitions of each land cover type of IGBP and the definition of vegetation types in the map of 'Vegetation of China', vegetation distribution regions and species components of community (table 4). Because better sources were available in China for urban and built-up areas and the emphasis of this study was on vegetation classification, urban and built-up land types were not specially classified in this study. Snow and ice were excluded for similar reasons. The savannas type was not included in both maps. Figure 7 shows the areal comparisons at the pixel level for classes that are merged into physiognomically similar groups. The best agreement is located in areas of the most homogeneous cover types such as barren or sparsely vegetated land (92.3%) (class 16), water bodies (90.1%) (class 17) and evergreen needle leaf forest (79.9%)

Table 2. Vegetation classification system. Codes in parenthesis are the same as the vegetation type numbers in figures 4 and 6 and table 1.

1. Forest
- 11 Evergreen forest
  - 111 Subtropical and tropical evergreen coniferous forest (18)
  - 112 Temperate and subtropical deciduous broadleaf forest (deciduous *Quercus*) + tropical evergreen broadleaf forest (10)
  - 113 Subtropical evergreen broad forest (9)
  - 114 Tropical evergreen broad rain forest (11)
- 12 Deciduous forest
  - 121 Cool temperate and temperate mountain deciduous coniferous forest (1)
  - 122 Temperate and subtropical deciduous broadleaf forest(5) (deciduous shaw)
  - 123 Temperate and subtropical deciduous broadleaf forest(deciduous *Quercus*) (6)
  - 124 Subtropical and tropical mountain deciduous broadleaf forest (3)
- 13 Mixed forest
  - 131 Temperate deciduous broadleaf forest + evergreen coniferous forest (4)
  - 132 Temperate and subtropical mountain deciduous leaflet forest (7)
  - 133 Subtropical evergreen and deciduous broadleaf mixed forest on mountain (mixed with shrub) (8)

2. Shrub and short forest
- 21 Evergreen, deciduous shrubbery and short forest
  - 211 Subtropical, tropical evergreen and deciduous shrub, short forest (19)
- 22 Deciduous Shrub
  - 221 Temperate and subtropical deciduous shrub, short forest (12) (*Corylus heterophylla, Lespedeza bicolor, Quercus mogolica*, etc.)
  - 222 Temperate and subtropical deciduous shrub, short forest (13) (mixed with crops)
  - 223 Temperate and subtropical deciduous shrub, short forest (14) (*Vitex negundo*, etc.)
  - 224 Subtropical deciduous shrub, short forest (15) (*Exochorda racemosa, Forsythia, Quercus variabilis*, etc.)
  - 225 Temperate and subtropical deciduous high-mountain shrub, short forest (20)

3. Grassland
- 31 Temperate grassland
  - 311 Meadow grassland (27) (*Filifolium sibiricum*)
  - 312 Meadow grassland (28) (*Leymus chinensis*)
  - 313 Typical grassland (30) (*Stipa grandis, Stipa kelillovi*)
  - 314 Typical grassland (31) (*Stipa krylovii, Cleistogenes squarrosa*)
  - 315 Mountain grassland (32)
  - 316 Desert grassland (33)
  - 317 Herbaceous swamp(41)
  - 318 Saline meadow (37)
- 32 Temperate and subtropical high and cold grassland
  - 321 High and cold grassland (35)
  - 322 High and cold grassland + meadow (36)
  - 323 High and cold (38) (*Gramineous ruderal*)
  - 324 High and cold meadow (39) (*Fleabane*)

4. Crop
- 41 Single crops and firgostabile economic crops (42)
- 42 Annually double crops or triple crops in 2 years (43)
- 43 Double cropping rice and annually triple crops, and subtropical evergreen economic forest and orchard (44)
- 44 Double cropping rice and tropical evergreen economic forest and orchard (45)

Table 2. (*Continued*).

5. Mixed types
- 51 Deciduous broadleaf shrub, short forest (sandy vegetation) + temperate typical grassland (16)
- 52 Evergreen and deciduous broadleaf shrub, short forest + meadow (17)
- 53 Evergreen and deciduous broadleaf shrub, short forest + meadow + crops (2)
- 54 Single crop + meadow grassland (29) (*Stipa baicalensis/Bothriochloa ischaemum, Themeda triandra*)
- 55 Subtropical and tropical mountain deciduous broadleaf forest + shrub + short forest (40)

6. Sparse vegetation and barren
- 61 Sparse vegetation
  - 611 Temperate short semi-shrub desert (21)
  - 612 Temperate short semi-shrub desert + shrub and semi-shrub desert (22)
  - 613 Temperate shrub and semi-shrub desert + semi-arbour desert (23)
  - 614 Temperate shrub and semi-shrub desert (24)
  - 615 Temperate semi-arbour desert (25)
  - 616 Temperate mountain short gramineous grassland + short semi-shrub desert (34)
  - 617 High and cold grovel semi-shrub desert (26)
- 62 Barren (46)

Table 3. Results of accuracy assessment.

Regions of GPS sampling	Input images	Total	Correct	Error	Mixed	Accuracy (%)
Hai Nan Province	NDVIs + PC1	131	88	30	13	67.2
	NDVIs	131	79	38	13	60.3
Northeast of China and	NDVIs + PC1	89	66	8	15	74.2
East of Inner Mongolia	NDVIs	89	67	6	16	75.3
Sinkiang and Qinghai	NDVIs + PC1	232	168	41	23	72.4
Province	NDVIs	232	124	108		53.4
Average	NDVIs + PC1					71.4
	NDVIs					63.0

'Total'—the total number of field sampling plots. 'Correct'—the number of plots where observed vegetation types are consistent with the classification result. 'Error'—those plots whose observed vegetation types are inconsistent with the classification results. 'Mixed' is a special type of error related to two scenarios: either the field observed data for a particular plot were a mosaic of a number of vegetation types and the area percentage of each type is less than 50%, or there was only one observed type in the field but classified as one of the 'Mixed' types as listed in table 2. 'Accuracy' was a ratio of 'Correct' and 'Total'.

(class 1). The greatest difference between the two classification systems appears in persistent wetlands (0.26%) (class 11). The majority of the confusion is related to physiognomically similar classes and classes representing mixed assemblages. The agreement level is relatively high for grasslands (class 10), croplands (class 12), evergreen broadleaf forest (class 2) and deciduous needle leaf forest (class 3).

Meadow grassland (class 8) and cropland/other vegetation mosaic (class 14) in our results are mainly confused with croplands (class 12) in the IGBP map. Such confusion exists among closed shrublands (class 6), croplands and cropland/other vegetation mosaic. It is very difficult to distinguish those types because of their physiognomical and regional similarity, and the disturbance of human activities. Herbaceous swamp (no. 41) and saline meadow (no. 37) in our map correspond to

Table 4. Conversion of our categories to IGBP DISCover land cover classification system.

Class	IGBP DISCover land cover classification system	Transformation of our classification system	Number of aggregation for vegetation types of our system
1	Evergreen Needleleaf Forest	Evergreen Coniferous Forest	18
2	Evergreen Broadleaf Forest	Evergreen Broadleaf Forest	9, 10, 11
3	Deciduous Needleleaf Forest	Deciduous Coniferous Forest	1
4	Deciduous Broadleaf Forest	Deciduous Broadleaf Forest	3, 5, 6, 40
5	Mixed Forests	Mixed Forests	4, 7, 12
6	Closed Shrublands	Closed Shrublands	8, 15, 19
7	Open Shrublands	Open Shrublands	14, 16, 17, 20, 24, 25
8	Woody Savannas	Meadow Grassland	27
9	Savannas		
10	Grasslands	Grasslands	28, 30, 31, 32, 33, 35, 36, 38, 39
11	Persistent Wetlands	Persistent Wetlands	37, 41
12	Croplands	Croplands	42, 43, 44, 45
13	Urban and Built-Up		
14	Cropland/Other Vegetation Mosaic	Mixed Types (Cropland/Other Vegetation Mosaic)	2, 13, 29
15	Snow and Ice		
16	Barren or Sparsely Vegetated	Sparse Vegetation and Barren	21, 22, 23, 26, 34, 46
17	Water	Water Body*	47

*Note: Water body is a separate type that is not listed in table 2.

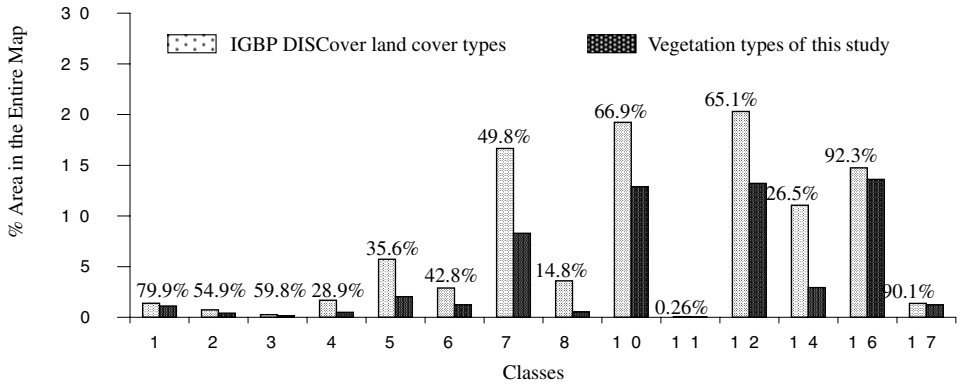

Figure 7. Percent distribution of IGBP DISCover land cover types and their areal comparison with results obtained in this study. 1 = Evergreen Needleleaf Forest; 2 = Evergreen Broadleaf Forest; 3 = Deciduous Needleleaf Forest; 4 = Deciduous Broadleaf Forest; 5 = Mixed Forests; 6 = Closed Shrublands; 7 = Open Shrublands; 8 = Woody Savannas; 10 = Grasslands; 11 = Persistent Wetlands; 12 = Croplands; 14 = Cropland/Other Vegetation Mosaic; 16 = Barren or Sparsely Vegetated; 17 = Water. Percentages on top of bars of the land cover classes indicate the level of agreement between the two maps for that particular class. Result of agreement validation can be divided into four groups, percent agreement I > 60% (classes 1, 10, 12, 16, 17), 60% > II (classes 2, 3, 6, 7) > 40%, 40% > III (classes 4, 5, 14) > 20% and IV (class 8) < 20%.

persistent wetlands (Class 11) in IGBP. They agree with the definition of persistent wetlands by IGBP, i.e. 'lands with a permanent mixture of water and herbaceous or woody vegetation that cover extensive areas. The vegetation can be present in either salt, brackish, or fresh water' (Hansen *et al.* 2000). It is necessary to verify them in the field.

Accuracy assessment was made again according to field observation to both the IGBP DISCover land cover map and the map aggregated from our previous vegetation classification map (table 5). The accuracy for the map of aggregation is higher than that for the IGBP DISCover land cover map. The overall classification accuracies of the two maps were 86.3% and 75.5%, respectively. An increase of 10.8% over the IGBP DISCover land cover map was achieved here.

Table 5. Accuracy assessment results from the aggregated vegetation map and the IGBP DISCover land cover map.

Regions of GPS sampling	Input images	Total	Correct	Error	Mixed	Accuracy (%)
Hai Nan Province	NDVIs + PC1	131	110	19	2	84.0
	IGBP	131	90	41		68.7
Northeast of China and	NDVIs + PC1	89	83	2	4	93.3
East of Inner Mongolia	IGBP	89	73	5	11	82.0
Sinkiang and Qinghai	NDVIs + PC1	232	189	41	2	81.5
Province	IGBP	232	176	56		75.9
Average	NDVIs + PC1					86.3
	IGBP					75.5

6. Discussion and conclusions

Based on our experiments, the multi-temporal NOAA AVHRR NDVI images record reliable seasonal rhythm of plant growth. Bio-temperature, potential evapotranspiration rate of Holdridge's life zone are helpful in improving vegetation classification when coupled with multi-temporal NDVI data.

In this study, vegetation–climate indices derived from Holdridge's life zone were combined with 1 km multi-temporal NOAA AVHRR NDVI images in vegetation classification. The inclusion of the climate information improved the average classification from 63.3% by using the NDVI images alone to 71.4% based on validation sites established in the field using GPS. This indicates that Holdridge's life zone is a useful vegetation–climate system applicable to global vegetation classification.

Our results compared favourably with the IGBP classification results. By crosswalking our classification results into the IGBP DISCover land cover classification system, we obtained an aggregated vegetation map. The overall classification accuracies for the aggregated vegetation map and the IGBP land cover map were 86.3% and 75.5%, respectively. We attribute the classification improvement in our results partially to the inclusion of the climate data summarized by the climate–vegetation indices based on Holdrige's life zone classification. Such indices can be generated as quantitative parameters for large area vegetation classification. It helps to reduce the confusions among different vegetation classes with similar seasonal NDVI rhythms.

In addition to Holdridge's life zone system, there also exist some other analogous classification systems, for example, Penman (1956) and Thornthwaite (1948). They may be synthetically utilized in classification of global land cover types along with remotely sensed data. Their potential needs to be further assessed.

All classification accuracies reported in this paper are based on a limited set of field validation samples due to cost reasons. As more validation samples are being collected, more extensive evaluation of various classification algorithms will be carried out in the future.

Acknowledgements

This study was funded by the Natural Science Foundation of China (39899374, 49825511 and 30000027) and Project of Foundation for University Key Teacher by Ministry of Education. Institute of Resource Science of Beijing Normal University (BNU), Key Laboratory of Environmental Change and Natural Disaster of Beijing Normal University, Ministry of Education of China and CAMFER at the University of California at Berkeley have provided equipment used in this study. We would like to thank USGS EROS Data Center for providing 1 km NOAA AVHRR NDVI images and DEM data, and the Climate Center of State Meteorological Administration of China for providing climate data. We are grateful to Prof. Muyi Kang, Yuan Jiang, Institute of Resource Science of BNU for their advice and help on the methods and theory of this study.

References

Achard, F., and Estreguil, C., 1995, Forest classification of southeast Asia using NOAA AVHRR data. *Remote Sensing of Environment*, **54**, 198–208.

Asrar, G., and Dozier, J., 1994, EOS: science strategy for the earth observing system. NASA, AIP Press.

Box, E., Holben, B. N., and Kalb, V., 1989, Accuracy of AVHRR vegetation index as a predictor of biomass, primary productivity and net CO_2 flux. *Vegetatio*, **80**, 71–89.

Belward, A. S. (ed.), 1996, The IGBP-DIS Global 1 km Land Cover Data Set 'DISCOVER': proposal and implementation plans. Report WP no. 13, IGBP-DIS, Stockholm, Sweden.

Brown, J. F., Loveland, T. R., Merchant, J. W., Reed, B. C., and Ohlen, D. O., 1993, Using multisource data in global land characterization: concepts, requirements, and method. *Photogrammetric Engineering and Remote Sensing*, **59**, 977–987.

Chang, Hsin-shih, 1989, The potential evapotranspiration (PE) index for vegetation and vegetation–climatic classification (II)—an introduction of main methods and PEP program. *Acta Phytoecologica et Geobotanica Sinica*, **13**, 197–207 [In Chinese].

Chang, Hsin-shih, 1993, The potential evapotranspiration (PE) index for vegetation and vegetation–climatic classification (III)—an introduction of main methods and PEP program. *Acta Phytoecologica et Geobotanica Sinica*, **17**, 97–109 [In Chinese].

Cihlar, J., Ly, H., and Xiao, Q., 1996, Land cover classification with AVHRR multichannel composites in northern environments. *Remote Sensing of Environment*, **58**, 36–51.

Cihlar, J., Xiao, Q., Beaubien, J., Fung, K., and Latifovic, R., 1998, Classification by Progressive Generalization: a new automated methodology for remote sensing multichannel data. *International Journal of Remote Sensing*, **19**, 2685–2704.

Cihlar, J., 2000, Land cover mapping of large areas from satellites: status and research priorities. *International Journal of Remote Sensing*, **21**, 1093–1114.

DeFries, R., and Townshend, J. R. G., 1994, NDVI-derived land cover classification at a global scale. *International Journal of Remote Sensing*, **15**, 3567–3586.

DeFries, R., Field, C., Fung, I., Justice, C., Los, C., Maston, P., Matthews, E., Mooney, H., Potter, C., Prentice, K., Sellers, P., Townshend, J., Ustin, S., and Vitousek, P., 1995a, Mapping the land surface for global atmosphere–biosphere models: toward continuous distributions of vegetation's functional properties. *Journal of Geophysical Research*, **100**, 20867–20882.

DeFries, R., Hansen, M., and Townshend, J., 1995b, Global discrimination of land cover types from metrics derived from AVHRR Pathfinder data. *Remote Sensing of Environment*, **54**, 209–222.

DeFries, R., Townshend, J. R., G., and Hansen, M., 1998a, Continuous fields of vegetation characteristic at the global scale. *Journal of Geophysical Research*, **104**, 16911–16923.

DeFries, R. S., Hansen, M. C., Townshend, J. R. G., and Sohlberg, R. S., 1998b, Global land cover classification at 8 km spatial resolution: the use of training data derived from Landsat imagery in decision tree classifiers. *International Journal of Remote Sensing*, **19**, 3141–3168.

Driese, K. L., Reiners, W. A., Merrill, E. H., and Gerow, K. G., 1997, A digital land cover map of Wyoming, USA: a tool for vegetation analysis. *Journal of Vegetation Science*, **8**, 133–146.

Eastman, R. J., and Fulk, M., 1993, Long sequence time series evaluation using standardized principal components. *Photogrammetric Engineering and Remote Sensing*, **59**, 1307–1312.

Eidenshink, J. C., 1992, The 1990 conterminous US AVHRR data sets. *Photogrammetric Engineering and Remote Sensing*, **58**, 809–813.

El Saleous, N. Z., Vermote, E. F., Justice, C. O., Townshend, J. R. G., Tucker, C. J., and Goward, S. N., 2000, Improvements in the global biospheric record from the Advanced Very High Resolution Radiometer (AVHRR). *Remote Sensing of Environment*, **21**, 1251–1277.

Fung, T., and LeDrew, E., 1987, Application of principal components analysis to change detection. *Photogrammetric Engineering and Remote Sensing*, **53**, 1649–1658.

Gong, P., 1993, Change detection using principal component analysis and fuzzy set theory. *Canadian Journal of Remote Sensing*, **19**, 22–29.

Goward, S. N., and Hope, A. S., 1989, Evapotranspiration from combined reflected solar and emitted terrestrial radiation: preliminary FIFE results from AVHRR data. *Advances in Space Research*, **9**, 239–249.

Hansen, M. C., and Reed, B., 2000, A comparison of the IGBP DISCover and University of Maryland 1 km global land cover products. *International Journal of Remote Sensing*, **21**, 1365–1373.

Hansen, M., Dubayah, R., and DeFries, R., 1996, Classification trees: an alternative to traditional land cover classifiers. *International Journal of Remote Sensing*, **17**, 1075–1081.

Hansen, M. C., DeFries, R. S., Townshend, J. R. G., and Sohlberg, R., 2000, Global land cover classification at 1 km spatial resolution using a classification tree approach. *International Journal of Remote Sensing*, **21**, 1331–1364.

Holdridge, L. R., 1947, Determination of world plant formation from simple climatic data. *Science*, **105**, 367–368.

Holdridge, L. R., 1967, *Life Zone Ecology*, revised edn (San Jose, Costa Rica: Tropical Science Center).

IGBP, 1990, The International Geosphere–Biosphere Programme: a study of global change—the initial core project. IGBP Global Change Report no. 12, International Geosphere–Biosphere Programme, Stockholm, Sweden.

IGBP, 1992, Improved Global Data for Land Applications, edited by J. R. G. Townshend. IGBP Global Change Report no. 20, International Geosphere–Biosphere Programme, Stockholm, Sweden.

Kramer, H. J., 1994, *Observation of the Earth and its Environment. Survey of Mission and Sensors*, 2nd edn (Berlin: Springer Verlag)

Lambin, E. F., and Ehrlich, D., 1995, Combining vegetation indices and surface temperature for land-cover mapping at broad spatial scales. *International Journal of Remote Sensing*, **16**, 573–579.

Laport, N. T., Goetz, S. J., Justice, C. O., and Heinecke, M., 1998, A new land cover map of central Africa derived from multi-resolution, multi-temporal AVHRR data. *International Journal of Remote Sensing*, **19**, 3537–3550.

Loveland, T. R., and Belward, A. S., 1997, The IGBP-DIS global 1 km land cover data set, DISCover: first results. *International Journal of Remote Sensing*, **18**, 3289–3295.

Loveland, T. R., Merchant, J. W., Ohlen, D. O., and Brown, J. F., 1991, Development of a land-cover characteristics database for the conterminous U.S. *Photogrammetric Engineering and Remote Sensing*, **57**, 1453–1463.

Loveland, T. R., Merchant, J. W., Brown, J. F., Ohlen, D. O., Reed, B. C., Olson, P., and Hutchinson, J., 1995, Seasonal land-cover regions of the United States. *Annals of Association of American Geographer*, **82**, 339–355.

Loveland, T. R., Reed, B. C., Brown, J. F., Ohlen, D. O., Zhu, Z., Yang, L., and Merchant, J. W., 2000, Development of a global land cover characteristics database and IGBP DISCover from 1 km AVHRR data. *International Journal of Remote Sensing*, **21**, 1303–1330.

Moody, A., 1998, Using landscape spatial relationships to improve estimates of land-cover area from coarse resolution remote sensing. *Remote Sensing of Environment*, **64**, 202–220.

Penman, H. L., 1956, Estimating evaporation. *Transactions of American Geographical Union*, **37**, 43–50.

Potter, C. S., Randerson, J. T., Field, C. B., Matson, P. A., Vitousek, P. M., Mooney, H. A., and Klooster, S. A., 1993, Terrestrial ecosystem production: a process model based on global satellite and surface data. *Global Biogeochemical Cycles*, **7**, 811–841.

Prince, S. D., 1991, A model of regional primary production for use with coarse-resolution satellite data. *International Journal of Remote Sensing*, **12**, 1313–1330.

Ruimy, A., Saugier, B., and Dedieu, G., 1994, Methodology for the estimation of terrestrial net primary production from remotely sensed data. *Journal of Geophysical Research*, **99**, 5263–5283.

Running, S. W., and Nemani, R. R., 1988, Relating seasonal patterns of the AVHRR vegetation index to simulated photosynthesis and transpiration of forests in different climates. *Remote Sensing of Environment*, **24**, 347–367.

Running, S. W., Loveland, T. R., and Pierce, L. L., 1995, A vegetation classification logic for global land cover analysis. *Remote Sensing of Environment*, **51**, 39–48.

Sellers, P. J., 1985, Canopy reflectance, photosynthesis, and transpiration. *International Journal of Remote Sensing*, **6**, 1335–1372.

Thornthwaite, C. W., 1948, An approach toward a rational classification of climate. *Geographical Review*, **38**, 57–94.

Townshend, J. R. G., 1994, Global data sets for land applications from the advance very high resolution radiometer: an introduction. *International Journal of Remote Sensing*, **15**, 3319–3332.

Townshend, J. R. G., Justice, C. O., and Kalb V., 1987, Characterization and classification of South American land cover types using satellite data. *International Journal of Remote Sensing*, **7**, 1395–1416.

Townshend, J. R. G., Justice, C. O., Li, W., Gurney, C., and McManus, J., 1991, Global land cover classification by remote sensing: present capabilities and future possibilities. *Remote Sensing of Environment*, **35**, 234–255.

Tucker, C. J., Townshend, J. R. G., and Goff, T. E., 1985, African land-cover classification using satellite data. *Science*, **227**, 369–375.

Tucker, C. J., and Sellers, P., 1986, Satellite remote sensing of primary production. *International Journal of Remote Sensing*, **7**, 1395–1416.

Wu, Chuanjun, 1990, *1:1,000,000 Land Use Map of China* (Beijing: Science Press) [In Chinese].

Wu, Zhengyi (editor in chief), 1980, *Chinese Vegetation* (Beijing: Science Press) [In Chinese].

Xu, Wenduo, 1985, Quantity of heat indices of Kira and its application in vegetation of China. *Journal of Ecology*, **15(3)**, 35–39 [In Chinese].